Realistic Shell Model Interpretation for the Nuclear Structure of Some 1f-2p Shell Nuclei

Ehsan M. Raheem*, Ali A. Abdulhasan

Iraqi Atomic Energy Commission, Baghdad, Iraq

Author E-mail: ehsan.nucl@yahoo.com

https://doi.org/10.29072/basjs.20240105

ARTICLE INFO

Keywords

Shell model, Harmonic oscillator potential, Charge density distribution Electron scattering, Nuclear structure.

ABSTRACT

The charge density distributions (CDD), charge form factors, occupation numbers of states, and root mean square charge (rms_{ch}) radii, have been calculated for several *1f-2p* shell-model nuclei, such as ^{48}Ti, ^{50}Ti, ^{50}Cr, ^{52}Cr, ^{58}Ni, and ^{60}Ni nuclei using the wave functions for a single particle in a harmonic oscillator (HO) potential. The size parameter *b* of the HO potential is considered as a free parameter chosen to reproduce the rms_{ch} radii. The nuclear real states occupation numbers have been assumed to differ from the simple shell model predictions. Introducing extra parameters such as σ_1 and σ_2 to characterize the disparity between the occupation numbers of real states and those anticipated by the simple shell model, leads to achieving a high level of agreement between the calculations and experimental data. Obtained results lead to the conclusion that the proposed parameters σ_1 and σ_2, bring the calculated CDD and form factors closer to the experimental data along with all values of radius *r* and momentum transfer *q*, respectively.

Received 07 Oct 2023; Received in revised form 21 Apr 2024; Accepted 27 Apr 2024, Published 30 Apr 2024

1. Introduction

Electron scattering from nuclei [1-3] has shown to be one of the most efficient methods for researching the nuclear structure. This method has been recognized as an efficient way to obtain crucial information regarding the size of the nucleus and the spatial distributions of its charge, current, and magnetization [4]. The cross-section of the target nucleus, as measured, can directly correspond to the matrix elements of these quantities and the structure of the target nucleus [5]. The measurements of electron scattering can be performed without affecting the structure of the target because the interaction is weak and well-known [6]. This concept is in contrast to the case of using nucleon scattering from nuclei, where the mechanism of the interaction cannot be separated from the structural effects of the target. The information magnitude deduced by the electron scattering measurements depends on the de Broglie wavelength of the incident electron. This wavelength is associated with the incident electron energy. Electron energy must be equal to or more than 100 MeV to bring the de Broglie wavelength within the spatial dimensions of the target nucleus [7] and thus compiling accurate information about the nuclear structure of the investigated nucleus. The nuclear size is associated with the nuclear form factor, which relies on the distribution of current, charge, and magnetization within the target nucleus. The form factor of the nucleus is embedded within the measured cross-section and can be experimentally determined by considering the momentum transfer q if the scattered angle and the energies of the incident and scattered electrons are known. Gul'karov et al. [8] have proposed a simple method of calculation of the CDD for the nuclei in *sp* and *sd* shell. The HO wave functions beside the fractional filling numbers of states were used to calculate the CDD of ^{12}C, ^{16}O, ^{18}O, ^{24}Mg, ^{28}Si, $^{32,\ 34}$S, and ^{40,48}Ca nuclei. The additional parameter α, was included in calculations and a good agreement was achieved between the CDD and model-independent results along all values of r. This method has been adopted by several studies to investigate the nuclear ground-state properties such as the occupation numbers, root mean square (rms) radii, CDD, and related form factors for *1p*-shell nuclei [9], *1d-2s* shell nuclei [10-12], and *1f-2p* shell nuclei [13,14]. The present work is devoted to investigating the rms charge radii, occupation numbers of states, CDD, and elastic form factors for ^{48,50}Ti, ^{50,52}Cr, and ^{58,60}Ni nuclei using the Gul'karov method [8] that has been extended to include *1f-2p* shell.

2. Theory

In the context of the harmonic oscillator (HO) wave functions, it is possible to determine the CDD by [8, 15]:

$$\rho_{ch}(r)=\frac{1}{4\pi}\sum_{nl}(2j+1)\left|R_{nl}(r)\right|^2 \tag{1}$$

where $R_{nl}(\mathrm{r})$ is the radial part of the HO wave function, which is given by [16]:

$$R_{nl}^{r}=\left[(\pi^{1/2}b^{3})\{(2l+1)!!\}^{2}(2n-1)!\right]^{-1}2^{l-n+3}(2l+2n-1)!!\left(\frac{r}{b}\right)^{2l}$$

$$\cdot\sum_{k=0}^{n-1}\left[(-1)^{k}\{(\mathrm{n}-1-k)!\,k!\,(2k+2l+1)!!\}^{-1}2^{k}(n-1)!(2l+1)!!\left(\frac{r}{b}\right)^{2k}\right]^{2}e^{-r^{2}/b^{2}} \tag{2}$$

According to the simple shell model predictions, protons are distributed within the *1f-2p* shell in the following manner: there exists an inert core comprising fully occupied *1s*, *1p*, *1d*, and *2s* orbits, while (Z-20) protons occupy the *1f* orbit. So, from the equations (1) and (2), one can get:

$$\rho_{ch}(r)=\frac{4}{\pi^{3/2}b^{3}}\left\{\frac{5}{4}+\left(\frac{r}{b}\right)^{4}+\frac{2}{105}Z\left(\frac{r}{b}\right)^{6}-\frac{8}{21}\left(\frac{r}{b}\right)^{6}\right\}e^{-r^{2}/b^{2}} \tag{3}$$

where *b* is the HO size parameter.

The mean square charge radii (MSR) is given by [17, 18]:

$$\left\langle r^{2}\right\rangle=\frac{4\pi}{Z}\int_{0}^{\infty}\rho_{ch}(r)r^{4}dr \tag{4}$$

and the normalization of the CDD is given by [19]:

$$Z=4\pi\int_{0}^{\infty}\rho_{ch}(r)r^{2}dr \tag{5}$$

From the equations (3) and (4), one can get the MSR of the considered *1f-2p* shell nuclei as:

$$\left\langle r^{2}\right\rangle=\frac{b^{2}}{Z}\left(\frac{9}{2}Z-30\right) \tag{6}$$

Due the insufficient agreement between the calculated CDD using the basic shell model outlined in equation (3) and data from experiments, an alternative method for calculating CDD is suggested. In real nuclear states, this alternative assumes that the *1s*, *1p*, and *1d* core orbits are filled by 2, 6, and 10 protons, respectively, while the remaining protons are distributed over

2s, *1f* and *2p* orbits with $(2-\sigma_1)$, $(Z-20-\sigma_2)$ and $(\sigma_1+\sigma_2)$ protons, respectively. Hence, the CDD for *1f-2p* shell is represented by:

$$\rho_{ch}(r)=\frac{1}{\pi^{3/2}b^3}\left\{5-\frac{3}{2}\sigma_1+\left[\frac{11}{3}\sigma_1+\frac{5}{3}\sigma_2\right]\left(\frac{r}{b}\right)^2+\left[4-2\sigma_1-\frac{4}{3}\sigma_2\right]\left(\frac{r}{b}\right)^4\right.$$

$$\left.+\left[\frac{8}{105}Z-\frac{32}{21}-\frac{8}{105}\sigma_2+\frac{4}{15}\sigma_1+\frac{4}{15}\sigma_2\right]\left(\frac{r}{b}\right)^6\right\}e^{-r^2/b^2} \quad (7)$$

where the parameter σ that equals to $(\sigma_1+\sigma_2)$, represents the difference between the occupation numbers in real nuclei and the simple shell model predictions. From equations (4) and (7), the MSR becomes:

$$\left\langle r^2\right\rangle=\frac{b^2}{Z}\left(\frac{9}{2}Z-30+\sigma_1\right) \quad (8)$$

The central CDD at *r*= 0 is given according to equation (7) by:

$$\rho_{ch}(0)=\frac{1}{\pi^{3/2}b^3}\left(5-\frac{3}{2}\sigma_1\right) \quad (9)$$

where the parameter σ_1 can be obtained from equation (9), after slight rearrangement, as:

$$\sigma_1=\frac{2}{3}\left(5-\rho_{ch}(0)\pi^{3/2}b^3\right) \quad (10)$$

where the values of $\rho_{ch}(0)$ are known and can be taken from experiments and *b* are chosen to reproduce the experimental rms_{ch}. The σ_2 represents a free parameter that is chosen to get the accordance between the calculated and experimental CDD. If $\sigma=\sigma_1=\sigma_2=0$, the obtained results of equations (7) and (8) are equal to the obtained results of equations (3) and (6), respectively.

In plane-wave Born approximation (PWBA) [20], the elastic electron scattering form factors from spin-zero nuclei can be determined using the Fourier transform of the CDD, and vice versa [21, 22]. Thus:

$$F(q)=\frac{4\pi}{Z}\int_0^\infty \rho_{ch}(r)\,j_0(qr)\,r^2\,dr \quad (11)$$

Here, $j_0(qr)=\sin(qr)/qr$ represents the zeroth-order spherical Bessel function. Therefore, equation (11) can be expressed as:

$$F(q)=\frac{4\pi}{qZ}\int_0^{\infty}\rho_{ch}(r)\,\sin(qr)\,r\,dr \tag{12}$$

To acquire the form factors for *1f-2p* shell nuclei, equation (7) for the CDD can be incorporated into equation (12) as:

$$F(q)=\frac{e^{-q^2b^2/4}}{Z}\left\{Z+\left[\frac{(10-Z)}{2}-\frac{\sigma_1}{6}\right](qb)^2+\left[\frac{(Z-15)}{20}+\frac{\sigma_1}{20}+\frac{\sigma_2}{24}\right](qb)^4\right.$$
$$\left.+\left[\frac{(20-Z)}{840}-\frac{\sigma_1}{240}-\frac{\sigma_2}{336}\right](qb)^6\right\}F_{cm}(q)\cdot F_{fs}(q) \tag{13}$$

Here, $F_{cm}(q)$ denotes the correction for the center of mass, while $F_{fs}(q)$ representing the correction for the finite size of nucleons. The both corrections are given by [23]:

$$F_{cm}(q)=\mathrm{e}^{q^2b^2/4A} \tag{14}$$

$$F_{fs}(q)=\mathrm{e}^{-0.43\,q^2/4} \tag{15}$$

where the nucleus mass number is denoted by *A*.

3. Results and discussion

The size parameter values for the considered nuclei are chosen to reproduce the experimental $\mathrm{rms}_{\mathrm{ch}}$ radii using equation (8). The values of σ_1 used in equation (8) are calculated using equation (10), where the central CDD $\rho_{ch}(r=0)$ are obtained from experimental data cited in Ref. [17]. The $\mathrm{rms}_{\mathrm{ch}}$ radii are calculated with and without σ_1 values using equations (8) and (6), respectively. The σ_2 values are considered as free parameters chosen to reproduce the experimental results of the CDD. The calculated values are presented in Table-1 alongside the experimental values. The calculated values of $\mathrm{rms}_{\mathrm{ch}}$ radii with $\sigma_1\neq 0$ are very close to the experimental values compared to those calculated with $\sigma_1=0$. Incorporating σ_1 parameters into the calculations results in a high favorable alignment between the calculated $\mathrm{rms}_{\mathrm{ch}}$ radii and experimental measurements, consequently leading to the selection of realistic and effective size parameter *b* values for the studied nuclei. The present work considered the studied nuclei consisting of a filled core of *1s*, *1p,* and *1d* orbits with 2, 6, and 10 protons, respectively. Other orbits such as *2s*, *1f*, and *2p* are considered to be occupied by $(2-\sigma_1)$, $(\mathrm{Z}-20-\sigma_2)$ and

$(\sigma = \sigma_1 + \sigma_2)$, respectively. Table-2 contains all calculated proton occupation numbers of the orbits outside the filled core for each isotope.

Table 1: Calculated size parameters *b*, rms_{ch} radii, σ_1 and σ_2 for *1f-2p* shell nuclei, alongside experimental values for rms_{ch} radii and central CDD at *r*=0.

Nucleus	Z	*b* (fm)	$\langle r^2 \rangle^{1/2}_{calc.}$ (fm) Eq.(6) $(\sigma_1 = 0)$	$\langle r^2 \rangle^{1/2}_{calc.}$ (fm) Eq.(8) $(\sigma_1 \neq 0)$	$\langle r^2 \rangle^{1/2}_{exp.}$ (fm) [17]	$\rho_{exp.}(0)$ (fm^{-3}) [17]	σ_1	σ_2
^{48}Ti	22	2.02	3.577	3.601	3.597	0.0787958	0.921	0.174
^{50}Ti	22	2.00	3.542	3.564	3.572	0.0827655	0.874	0.324
^{50}Cr	24	2.02	3.642	3.664	3.662	0.0777930	0.952	0.188
^{52}Cr	24	2.01	3.624	3.645	3.643	0.0794942	0.936	0.279
^{58}Ni	28	2.03	3.759	3.775	3.769	0.0806858	0.825	0.001
^{60}Ni	28	2.04	3.777	3.793	3.797	0.0800473	0.808	0.087

Table 2: Calculated proton occupation numbers of the states outside the core.

Nucleus	Occupation Numbers of *2s* orbit $(2-\sigma_1)$	Occupation Numbers of *1f* orbit $(Z-20-\sigma_2)$	Occupation Numbers of *2p* orbit $(\sigma = \sigma_1 + \sigma_2)$
^{48}Ti	1.079	1.826	1.095
^{50}Ti	1.126	1.676	1.198
^{50}Cr	1.048	3.812	1.140
^{52}Cr	1.064	3.721	1.215
^{58}Ni	1.175	7.999	0.826
^{60}Ni	1.192	7.913	0.895

The calculated CDD according to equations (7) and (3) with and without the inclusion of σ_1 and σ_2 parameters, respectively, are presented in Figures 1(a)-1(f) and compared with the fitted to the experimental data of Model-Independent (MI) [17]. The obtained results are displayed using dashed curves for $\sigma = \sigma_1 = \sigma_2 = 0$ and solid curves for $\sigma \neq \sigma_1 \neq \sigma_2 \neq 0$, while filled circles represent the experimental data of MI. The radius *r* is considered up to 10 fm to display the theoretical results over a wide range. Evidently, the dashed curves demonstrate a significant lack of agreement with the experimental data, particularly at $r \leq 2.75$ fm. The

incorporation of σ_1 and σ_2 parameters in the calculated CDD, indicated by the solid curves, achieving high level of concordance with the experimental data. Thus, considering the parameters σ_1 and σ_2, leads to an improvement in the CDD calculations and makes them more accurate compared to simple shell model calculations that neglect the effects of these parameters. Consequently, the higher orbits occupation numbers have the effects of reducing the CDD at the central regions, where charges are redistributed from these regions to the surface and the tail regions. Thus, the calculated rms_{ch} radii with σ_1 parameters are slightly larger than those calculated without these parameters or, in other words, without accounting for the effects of the higher orbits, as shown explicitly in Table-1. For the nuclei ^{48}Ti, ^{50}Ti, ^{50}Cr and ^{52}Cr, there are slight deviations between the solid curves and experimental data in the central regions, ranging from $r \approx 0.5$ fm to $r \approx 2.5$ fm, where the calculations overestimate the data. These deviations may be overcome by considering additional orbits such as *1g* or *2d* or *3s* to achieve exact agreement between the calculation and experimental results. Nevertheless, these deviations do not significantly affect the significant agreement obtained across most of the radius *r*. Electron scattering experiments enable a direct correlation between the scattering cross sections and the current, charge, and magnetization densities, offering valuable insights into the nuclear structures [23]. The CDD and their associated form factors provide a thorough comprehension of the spatial distribution of nuclear charge, and both quantities contain equivalent data amount. By employing the Fourier transform of the CDD, the elastic charge form factors can reveal the internal structure of the nuclei [24]. The calculated elastic charge form factors, with σ_1 and σ_2 parameters, are presented in Figures 2(a)-2(f) as a function of momentum transfer *q*. The calculations are represented by solid lines, while the experimental data of MI [17] are denoted by filled circles. There are very good agreements between the calculations and experimental data for momentum transfer values up to $q \approx 1.90$ fm^{-1}, $q \approx 1.80$ fm^{-1}, $q \approx 1.9$ fm^{-1}, $q \approx 1.80$ fm^{-1}, $q \approx 2.55$ fm^{-1}, and $q \approx 2.50$ fm^{-1} for ^{48}Ti, ^{50}Ti, ^{50}Cr, ^{52}Cr, ^{58}Ni, and ^{60}Ni, respectively. The calculated results describe the positions of the first diffraction minima accurately for all nuclei, as well as the second diffraction minima for ^{58}Ni and ^{60}Ni nuclei. However, for higher values of *q*, deviations between the calculations and experimental results become noticeable.

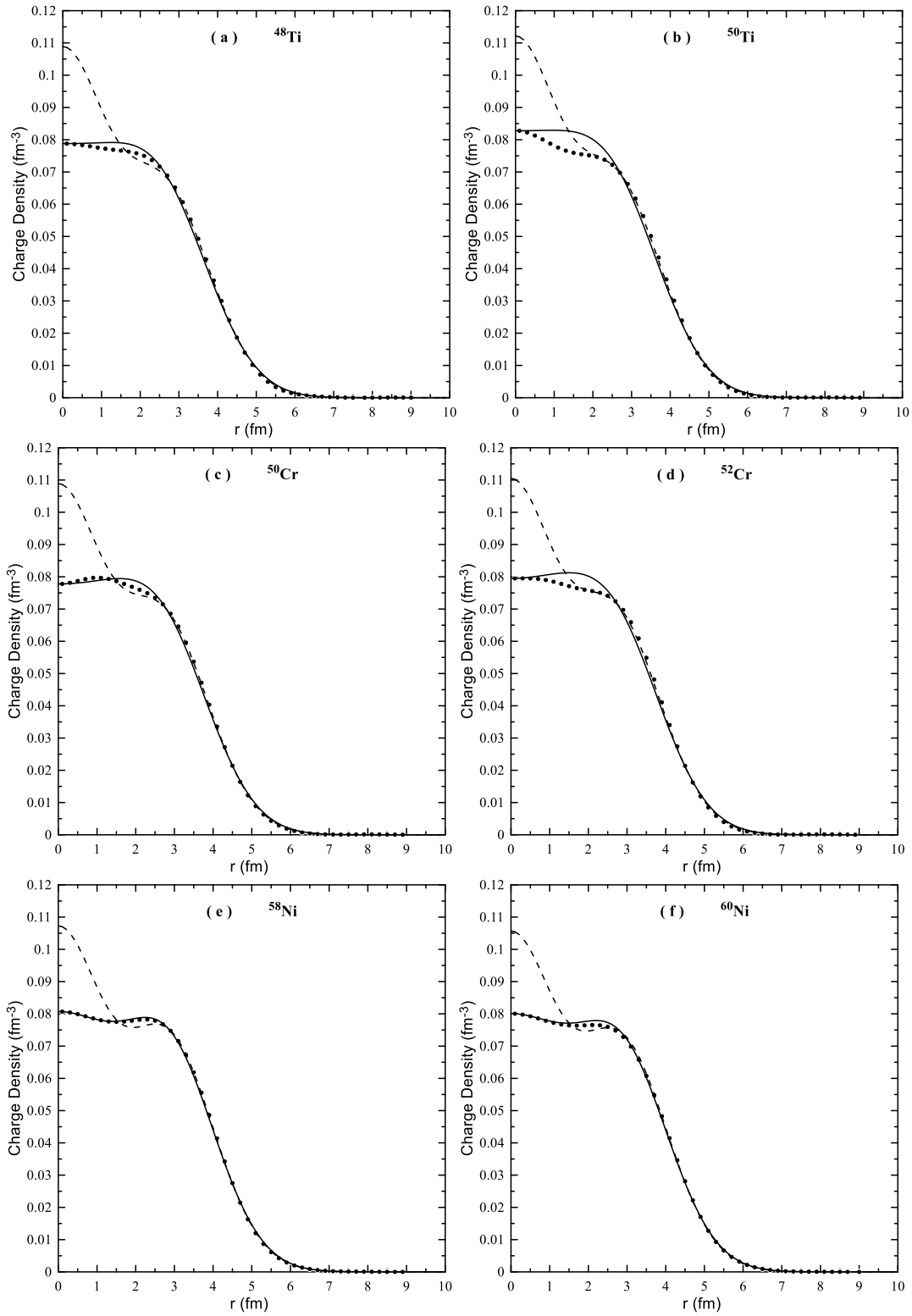

Figure 1: The CDD for ^{48,50}Ti, ^{50,52}Cr, and ^{58,60}Ni nuclei. The dashed curves, solid curves, and filled circles are the calculations with $\sigma = \sigma_1 = \sigma_2 = 0$, the calculations with $\sigma \neq \sigma_1 \neq \sigma_2 \neq 0$, and the experimental data of MI [17], respectively.

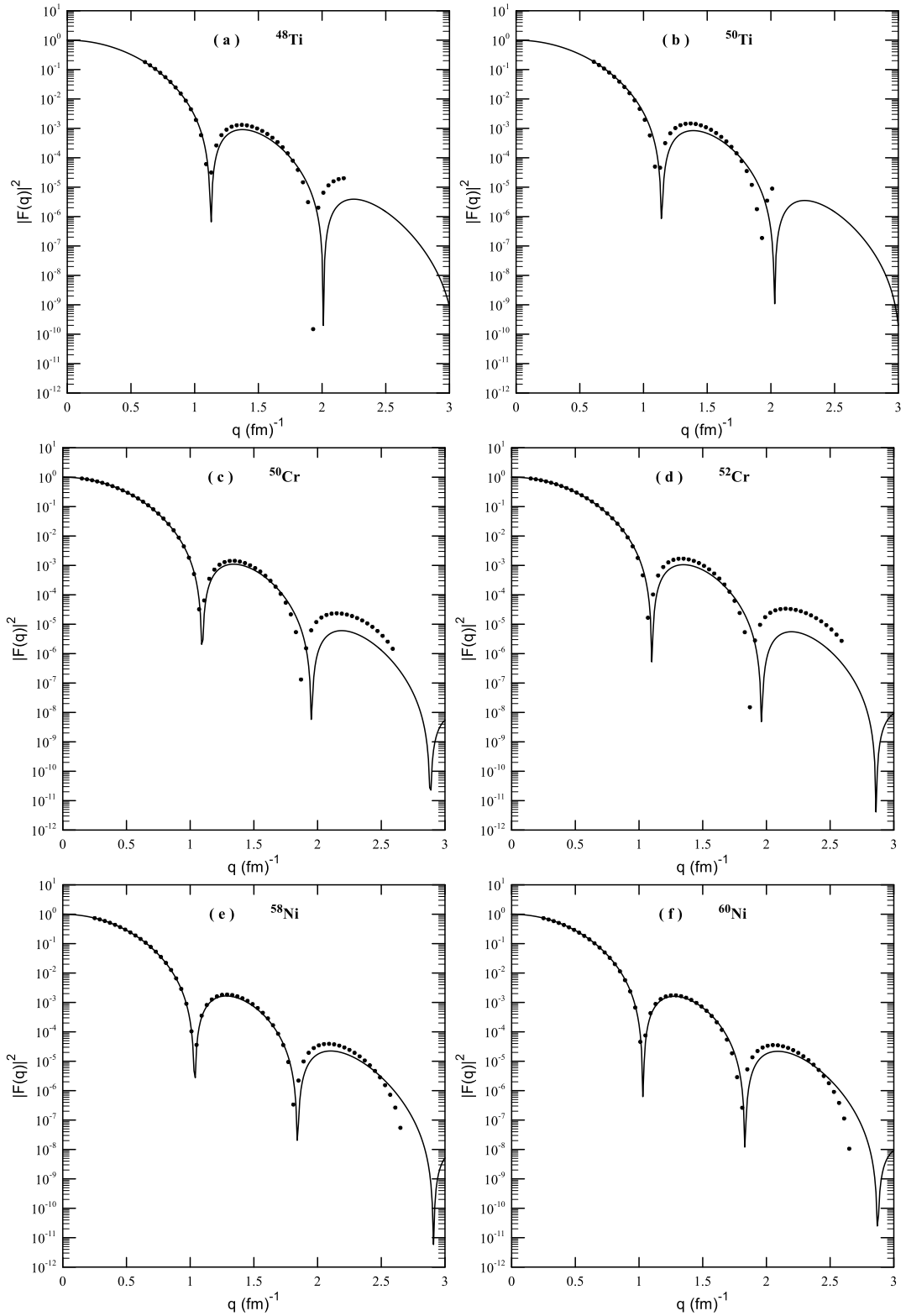

Figure 2: The elastic charge form factors for ^{48,50}Ti, ^{50,52}Cr, and ^{58,60}Ni nuclei. The solid curves, and filled circles represent the calculations with $\sigma \neq \sigma_1 \neq \sigma_2 \neq 0$, and the experimental data of MI [17], respectively.

4. Conclusions

In accordance with predictions of the simple shell model, the obtained results lead us to conclude that the calculated rms_{ch} radii, CDD, and the associated form factors for the nuclei ^{48,50}Ti, ^{50,52}Cr, and ^{58,60}Ni, exhibit notable deviations from the experimental data. Subsequently, the calculations have been adjusted through the introduction of supplementary parameters, denoted as σ_1 and σ_2, which are designated to account for the occupation numbers associated with the *2p* orbit in real nuclei. This strategic adjustment results in an impressive degree of concordance with the experimental rms_{ch} radii and concurrently leads to a reduction of the calculated CDD within central regions. The results show significant agreement with the experimental data in these specific regions, as well as across all values of *r*. Elastic electron scattering form factors have been calculated using σ_1 and σ_2 parameters, and the obtained results exhibit a commendable alignment with the experimental data.

References

[1] A. Richter, Electron scattering and nuclear structure at the S-DALINAC, Prog. Part. Nucl. Phys., 44 (2000) 3-28. https://doi.org/10.1016/S0146-6410(00)00053-3

[2] T. Suda, M. Wakasugi, Structure studies of unstable nuclei by electron scattering, Prog. Part. Nucl. Phys., 55 (2005) 417-436. https://doi.org/10.1016/j.ppnp.2005.01.008

[3] P. Sarriguren, Elastic Electron Scattering from Deformed and Oriented Odd-A Nuclei, Phys. Rev. C, 109 (2024) 024312. https://doi.org/10.1103/PhysRevC.109.024312

[4] B. Hernández, P. Sarriguren, O. Moreno, E. Moya de Guerra, D. N. Kadrev, A. N. Antonov, Nuclear shape transitions and elastic magnetic electron scattering, Phys. Rev. C, 103 (2021) 014303. https://doi.org/10.1103/PhysRevC.103.014303

[5] T. W. Donnelly, J. D. Walecka, Elastic magnetic electron scattering and nuclear moments, Nucl. Phys. A, 201 (1973) 81-106. https://doi.org/10.1016/0375-9474(73)90689-1

[6] J. D. Walecka, Electron scattering, Nucl. Phys. A, 574 (1994) 271C-296C. https://doi.org/10.1016/0375-9474(94)90050-7

[7] R. R. Roy, B. P. Nigam, Nuclear Physics: Theory and Experiment, John Wiley and Sons, New York, 1967.

[8] I. S. Gul'karov, M. M. Mansurov, A. A. Khomich, Charge density distribution of the 1s-1p and 1d-2s shell nuclei and filling numbers of the state, Sov. J. Nucl. Phys., 47 (1988) 25. https://api.semanticscholar.org/CorpusID:91959996

[9] A. K. Hamoudi, M. A. Hasan, A. R. Ridha, Nucleon momentum distributions and elastic electron scattering form factors for some 1p-shell nuclei, Pramana- J. Phys., 78 (2012) 737-748. https://doi.org/10.1007/s12043-012-0269-6

[10] T. S. Kosmas, J. D. Vergados, Nuclear densities with fractional occupation probabilities of the states, Nucl. Phys. A, 536 (1992) 72-86. https://doi.org/10.1016/0375-9474(92)90246-G

[11] A. A. Al-Rahmani, Charge density distributions for odd-A of 2s-1d shell nuclei, Baghdad Sci. J., 7 (2010) 1028-1033. https://doi.org/10.21123/bsj.7.2.1028-1033

[12] A. A. Al-Rahmani, Nucleon momentum distributions and elastic electron scattering from ^{19}F, ^{25}Mg, ^{27}Al, and ^{29}Si nuclei, Indian J. Phys., 90 (2016) 461-467. https://doi.org/10.1007/s12648-015-0762-0

[13] A. N. Abdullah, Charge density Distributions and Elastic Electron Scattering from ^{58}Ni, ^{64}Zn, ^{70}Ge and ^{76}Se nuclei using the occupation numbers of the states, Diyala J. Pure Sci., 13 (2017) 75-85. https://doi.org/10.24237/djps.1302.165a

[14] Z. A. Abdul Muhsin, The study of nuclear structure for some nuclei, Iraqi J. Phys., 16 (2018) 59-65. https://doi.org/10.30723/ijp.v16i36.30

[15] L. A. Mahmood, G. N. Flaiyh, Study of the Static and Dynamic Nuclear Properties and Form Factors for Some Magnesium Isotopes $^{29-34}$Mg, Iraqi J. Phys., 19 (2021) 82-93. https://doi.org/10.30723/ijp.v19i49.663

[16] P. J. Brussaard, P. W. M. Glaudemans, Shell-model applications in nuclear spectroscopy, North-Holland publishing company, Amsterdam, 1977.

[17] H. De Vries, C. W. De Jager, C. De Vries, Nuclear charge-density-distribution parameters from elastic electron scattering, At. Data Nucl. Data Tables, 36 (1987) 495-536. https://doi.org/10.1016/0092-640X(87)90013-1

[18] S. A. Rahi, G. N. Flaiyh, Matter Density Distributions, Root-mean Square Radii and Elastic Electron Scattering Form Factors of Some Exotic Nuclei (^{17}B, ^{11}Li, ^{8}He), Iraqi J. Phys., 19 (2021) 60-69. https://doi.org/10.30723/ijp.v19i50.675

[19] A. N. Abdullah, Investigation of the Nuclear Structure for Some p-Shell Nuclei by Harmonic Oscillator and Woods-Saxon Potentials, Al-Nahrain J. sci., 20 (2017) 42-48. https://doi.org/10.22401/jnus.20.2.06

[20] L. R. Suelzle, M. R. Yearian, H. Crannell, Elastic Electron Scattering from Li^6 and Li^7, Phys. Rev., 168 (1967) 1414. https://doi.org/10.1103/PhysRev.162.992

[21] R. Anni, G. Co, P. Pellegrino, Nuclear charge density distributions from elastic electron scattering data, Nucl. Phys. A, 584 (1995) 35-59. https://doi.org/10.1016/0375-9474(94)00508-K

[22] H. K. Mahdi, A. N. Abdullah, Elastic Form Factors and Matter Density Distributions of Some Neutron-Rich Nuclei, Iraqi J. Phys., 20 (2022) 18-27. https://doi.org/10.30723/ijp.v20i4.1013

[23] B. A. Brown, R. Radhi, B. H. Wildenthal, Electric quadrupole and hexadecupole nuclear excitations from the perspectives of electron scattering and modern shell model theory, Phys. Rep., 101 (1983) 313-358. https://doi.org/10.1016/0370-1573(83)90001-7

[24] T. de Forest Jr., J. D. Walecka, Electron scattering and nuclear structure, Adv. Phys., 15 (1966) 1-109. https://doi.org/10.1080/00018736600101254

تفسير أنموذج القشرة الواقعي للتركيب النووي لبعض نظائر القشرة 1f-2p

احسان مشعان رحيم*، علي احمد عبدالحسن

هيئة الطاقة الذرية العراقية، بغداد، العراق

المستخلص

تم دراسة توزيعات كثافة الشحنة النووية، عوامل التشكل للاستطارة الالكترونية المرنة، اعداد انشغال الحالات النووية وانصاف اقطار الشحنة لبعض نوى انموذج القشرة النووية *1f-2p* مثل النوى ^{48}Ti، ^{50}Ti، ^{50}Cr، ^{52}Cr، ^{58}Ni و^{60}Ni باستخدام الدوال الموجية للجسيمة المنفردة التي حُسبت باستخدام جهد المتذبذب التوافقي. تم اعتبار متغير الحجم b لجهد المتذبذب التوافقي كمتغير حر تم اختياره لإعادة انتاج انصاف اقطار الشحنة بحيث تتوافق مع النتائج التجريبية. تم افتراض ان اعداد انشغال الحالات الواقعية النووية تختلف عن توقعات انموذج القشرة البسيط. تم افتراض معاملات إضافية يرمز لها بالرموز σ_1 و σ_2 وذلك لوصف الاختلاف بين اعداد انشغال الحالات الواقعية النووية عن تلك التي تنبأ بها انموذج القشرة البسيط. ان تلك المعاملات المقترحة أدت الى جعل نتائج توزيعات كثافة الشحنة النووية وعوامل التشكل المحسوبة أقرب الى النتائج العملية عبر جميع قيم نصف القطر r والزخم المنتقل q على التوالي.